Stem Cell Research 52 (2021) 102233

Contents lists available at ScienceDirect

Stem Cell Research

journal homepage: www.elsevier.com/locate/scr

In vivo regeneration of rat laryngeal cartilage with mesenchymal stem cells derived from human induced pluripotent stem cells via neural crest cells

Masayoshi Yoshimatsu [a], Hiroe Ohnishi [a], Chengzhu Zhao [b], Yasuyuki Hayashi [a], Fumihiko Kuwata [a], Shinji Kaba [a], Hideaki Okuyama [a], Yoshitaka Kawai [a], Nao Hiwatashi [c], Yo Kishimoto [a,*], Tatsunori Sakamoto [d], Makoto Ikeya [b], Koichi Omori [a]

[a] Department of Otolaryngology-Head and Neck Surgery, Graduate School of Medicine, Kyoto University, Kyoto, Japan
[b] Department of Clinical Application, Center for iPS Cell Research and Application, Kyoto University, Kyoto, Japan
[c] Department of Otolaryngology, Kyoto-Katsura Hospital, Kyoto, Japan
[d] Department of Otorhinolaryngology, Shimane University Faculty of Medicine, Shimane, Japan

ARTICLE INFO

Keywords:
Human iPS cells
Regeneration
Laryngotracheal cartilage
Mesenchymal stem cell
Neural crest cells
Hyaline cartilage

ABSTRACT

The laryngotracheal cartilage is a cardinal framework for the maintenance of the airway for breathing, which occasionally requires reconstruction. Because hyaline cartilage has a poor intrinsic regenerative ability, various regenerative approaches have been attempted to regenerate laryngotracheal cartilage. The use of autologous mesenchymal stem cells (MSCs) for cartilage regeneration has been widely investigated. However, long-term culture may limit proliferative capacity. Human-induced pluripotent stem cell-derived MSCs (iMSCs) can circumvent this problem due to their unlimited proliferative capacity. This study aimed to investigate the efficacy of iMSCs in the regeneration of thyroid cartilage in immunodeficient rats. Herein, we induced iMSCs through neural crest cell intermediates. For the relevance to prospective future clinical application, induction was conducted under xeno-free/serum-free conditions. Then, clumps fabricated from an iMSC/extracellular matrix complex (C-iMSC) were transplanted into thyroid cartilage defects in immunodeficient rats. Histological examinations revealed cartilage-like regenerated tissue and human nuclear antigen (HNA)-positive surviving transplanted cells in the regenerated lesion. HNA-positive cells co-expressed SOX9, and type II collagen was identified around HNA-positive cells. These results indicated that the transplanted C-iMSCs promoted thyroid cartilage regeneration and some of the iMSCs differentiated into chondrogenic lineage cells. Induced MSCs may be a promising candidate cell therapy for human laryngotracheal reconstruction.

1. Introduction

The larynx and trachea play crucial roles in breathing, swallowing, and phonation. In particular, the cartilage provides a structural framework and is critical for the maintenance of an open airway for breathing. However, the cartilaginous framework is occasionally damaged by trauma or resected due to stenotic lesions or malignant invasion (Christine M. Pauken et al., 2019). Large cartilaginous defects result in airway problems, and reconstruction of the cartilaginous framework is necessary for the recovery of larynx and trachea function (Albrecht and Ostrower, 2019; Chang et al., 2019). Due to its avascular nature, laryngotracheal hyaline cartilage exhibits poor intrinsic regenerative ability (Bhosale and Richardson, 2008; Chiang et al., 2016). Thus, various approaches for the regeneration of laryngotracheal cartilage have been investigated.

Autologous chondrocytes (ACs) (Na et al., 2019) and mesenchymal

Abbreviations: HNA, Anti-human nuclear antigen; ACs, Autologous chondrocytes; DPSC, Dental pulp stem cell; EGF, Epidermal growth factor; EB, Embryoid body; ECM, Extracellular matrix; FGF, Fibroblast growth factor; FACS, Fluorescence activated cell sorting; iMSCs, hiPSC-derived MSCs; iNCCs, hiPSC-derived NCCs; hiPSCs, Human induced pluripotent stem cells; ICC, Immunocytochemistry; IHC, Immunohistochemistry; C-iMSC, iMSC/extracellular matrix complex; MSCs, Mesenchymal stem cells; NCCs, Neural crest cells; NGFR, Nerve growth factor receptor; PIPAAm, Poly(*N*-isopropylacrylamide); RHOB, Ras homolog family member B; TFAP2A, Transcription factor activating protein-2α; X-SCID, X-linked severe combined immunodeficiency.

* Corresponding author at: Department of Otolaryngology Head and Neck Surgery, Graduate School of Medicine, Kyoto University, 54 Kawahara-cho, Shogoin, Sakyo-ku, Kyoto 606-8507, Japan.

E-mail addresses: m_yoshimatsu@ent.kuhp.kyoto-u.ac.jp (M. Yoshimatsu), y_kishimoto@ent.kuhp.kyoto-u.ac.jp (Y. Kishimoto).

https://doi.org/10.1016/j.scr.2021.102233
Received 20 October 2020; Received in revised form 21 January 2021; Accepted 4 February 2021
Available online 11 February 2021

stem cells (MSCs) (Hashimoto et al., 2019; Nejadnik et al., 2010; Wakitani et al., 2011) have been well investigated as cell sources for cartilage regenerative cell therapy, and their potential has been clinically proven. However, these sources have some limitations. Normal cartilage has to be sacrificed for the preparation and expansion of ACs, which can cause conversion to a fibroblastic phenotype (Ma et al., 2013; von der Mark et al., 1971). The characteristics of autologous MSCs are unique to the individual and the harvest site (Im Gun-Il et al., 2005; Wagner et al., 2008), and repeated passages can limit the proliferative capacity of MSCs (Kretlow et al., 2008).

Recently, human-induced pluripotent stem cells (hiPSCs) have been investigated for articular cartilage regeneration (Ko et al., 2014; Nejadnik et al., 2015; Rim et al., 2018; Uto et al., 2018; Xu et al., 2017; Yamashita et al., 2015; Zhu et al., 2016) due to their unlimited proliferative capacity. Given that some craniofacial cartilages, including thyroid cartilage are formed by MSCs differentiated from neural crest cells (NCCs) during embryonic development (la Noce et al., 2014; Tabler et al., 2017), induced MSCs through NCC intermediates may have the potential for chondrogenic differentiation. In fact, hiPSC-derived MSCs (iMSCs) differentiated through NCC intermediates have been reported to have the potential to differentiate toward chondrogenic lineage cells *in vitro* (Fukuta et al., 2014; Menendez et al., 2013). Further, the inalterability of differentiation and proliferative potential of the induced NCCs during maintenance and expansion culture may be beneficial for achieving cartilage regeneration (Fukuta et al., 2014).

Given the future clinical applications of hiPSCs, xeno-free/serum-free conditions are critical for eliminating the use of animal-derived materials, which carry the risks of zoonoses and xenogeneic immune reactions (Astori et al., 2016; de Sousa et al., 2006). However, the chondrogenic differentiation potency of iMSCs for laryngotracheal cartilage defect repair and the efficiency of deriving these cells from hiPSCs under xeno-free/serum-free conditions for cartilage regeneration *in vivo* remain unclear.

Here, we investigated the efficacy of iMSCs cultured under xeno-free/serum-free conditions for thyroid cartilage regeneration. Following the induction of iMSCs differentiated through NCC intermediates, we transplanted clumps of iMSC/extracellular matrix complex (C-iMSCs) (Kittaka et al., 2015) into defective thyroid cartilage of immunodeficient rats and histologically examined the survival of transplanted cells and cartilage regeneration.

2. Materials and methods

2.1. Induction of hiPSC-derived MSCs (iMSCs) differentiated through NCC intermediates

A hiPSC line, 1231A3 (Nakagawa et al., 2014), generated under feeder-free/xeno-free conditions, was cultured on an iMatrix-511 (Nippi, Tokyo, Japan)-coated cell culture plate in StemFit® AK03N (Ajinomoto, Tokyo, Japan), as described previously. This cell line was established by Kyoto University, derived from ePBMC® (purchased from Cellular Technology Limited (http://www.immunospot.com/). The induction of iMSCs through NCCs was performed under xeno-free/serum-free conditions, which is a modified version of a previously described protocol (Fukuta et al., 2014), the details of which are described in a preprint (Kamiya et al., 2020). In brief, NCCs were induced in StemFit Basic03 (Ajinomoto), which is comparable to AK03N minus FGF2, supplemented with 10 μM SB431542 (Selleck Chemicals, Houston, TX, USA) and 1 μM CHIR99021 (Axon Medchem, Groningen, the Netherlands) for 10 days. To purify NCCs, CD271-stained cells were separated using the BD FACS Aria II cytometer (BD Biosciences, San Jose, CA, USA). The robustness of the protocol was confirmed by inducing NCCs from multiple iPSC lines (1231A3, 1381A5, 1381B5, 1383D2, and 1383D10) (Kamiya et al., 2020). Following maintenance of purified hiPSC-derived NCCs (iNCCs) in StemFit Basic03 supplemented with 10 μM SB431542, 20 ng/mL EGF (R&D systems, a Bio-Techne brand, MN, USA), and FGF2 (Wako, Osaka, Japan) on fibronectin-coated plates, the cells were induced to differentiate into MSCs using MSC medium (PRIME-XV MSC Expansion XSFM, Irvine Scientific, CA, USA) by switching the medium. Then, iMSCs were imaged at 10%–20% confluency using a phase-contrast microscope (Nikon-eclipse Ti-S, Nikon Corporation, Tokyo, Japan) and an Olympus DP73 camera (Olympus, Japan). Following one passage, the iMSCs were expanded for flow cytometry and C-iMSC fabrication. To validate the reproducibility of iMSC differentiation through NCC intermediates, three independent inductions from 1231A3 were performed (Supplementary Fig. S1) and induced cells were evaluated for the presence of NCC and MSC markers.

2.2. Flow cytometry

After the induction of iNCCs, 1.0×10^7 cells/mL in a single-cell suspension in FACS buffer (0.1% bovine serum albumin [BSA] in phosphate buffered saline [PBS]) were incubated with APC-conjugated anti-CD271 antibody (Table S1) for 30 min at 4 °C. After washing, the cells were re-suspended in FACS buffer. The cells were sorted using a BD FACS Aria II. Bimodal cell populations were observed, indicating the presence of populations with different APC-intensities. The $CD271^{high}$ population was sorted (Fig. 1-A-b) according to a previous report (Kamiya et al., 2020), in which $CD271^{high}$ cells, including a relative enrichment of NCCs, expressed NCC markers such as SOX10, NGFR, TFAP2A, and RHOB.

After iMSC induction, a Human MSC Verification Flow Kit (Supplementary Table S1, Cat: FMC020, R&D system) was used to confirm that the cells expressed characteristic MSC surface markers (CD90 and CD105) and lacked hematopoietic markers (CD45, CD34, CD79A, HLA-DR, and CD11b). CD73, detected using PE-conjugated anti-human CD73 (Table S1), was used as another MSC surface marker. The single-cell suspension (2.0×10^5 cells) in 100 μL of FACS buffer was incubated with these antibodies for 40 min at room temperature. After washing, the cells were re-suspended in FACS buffer. The cells were analyzed using a BD LSRFortessa Cell Analyzer (BD Biosciences) and Single-Cell Analysis Software FlowJo (Tree Star Inc., OR, USA). In all the MSC evaluation experiments, flow cytometry histograms of cells incubated with isotype controls (Table S1) were used as control populations.

2.3. Fabrication of C-iMSCs

For C-iMSC formation, 5.0×10^4 iMSCs/well were seeded onto 1.5 μg/cm^2 fibronectin (Millipore, CA, USA)-coated temperature-responsive 96-well plates (Upcell, CellSeed, Tokyo, Japan) containing MSC medium. In these commercially available temperature-responsive 96-well plates, 1.6 μg/cm^2 polymer poly(*N*-isopropylacrylamide) (PIPAAm) was grafted onto the tissue culture polystyrene surface. In response to lowering the temperature from 37 °C to room temperature, the cell-adhesive characteristic changed from cell-adhesive to cell-repellent with increasing PIPAAm graft density (Akiyama et al., 2014). On Day 5, the cell sheet was incubated at room temperature for 15 min, at which point the sheets spontaneously detached from the wells and were transferred onto low-attachment 96-well plates (Prime surface 96U plate, Sumitomo Bakelite, Tokyo, Japan). Then, the C-iMSCs were obtained on Day 7 (Fig. 2-A). Phase-contrast images of C-iMSCs were obtained using a phase-contrast microscope (Nikon-eclipse Ti-S), and the diameter of 75 C-iMSCs were measured using the cellSens Standard software (version 1.11, Olympus).

2.4. Animals

A total of 14 8-week-old X-linked immunodeficient (X-SCID) rats were provided by NBRP-Rat with support in part by the National Bio-Resource Project (NBRP), Japan. Animals were cared for in the Institute of Laboratory Animals of the Graduate School of Medicine, Kyoto University, Japan. All experimental procedures were performed under

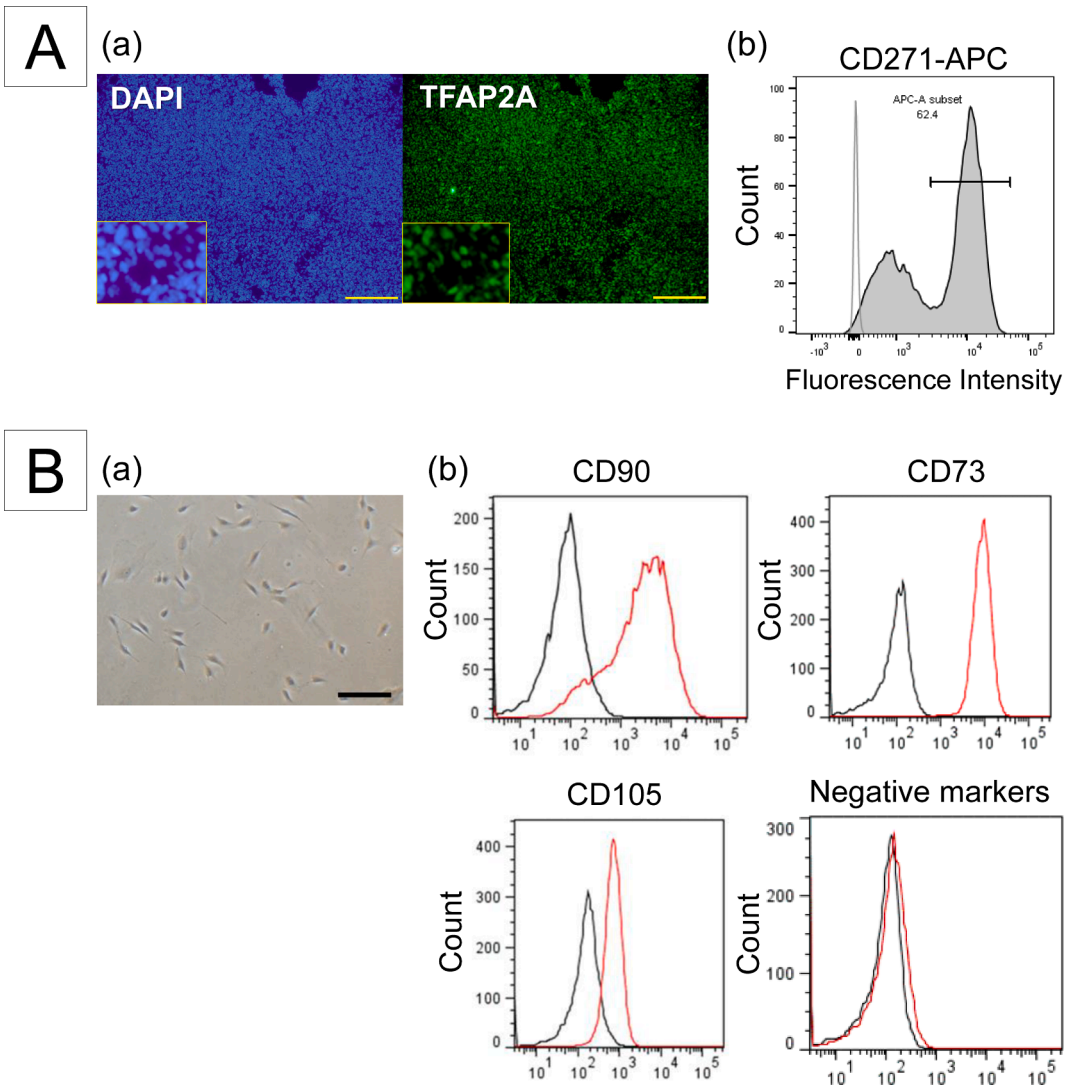

Fig. 1. Evaluation of hiPSC-derived neural crest cells (iNCCs) **(A)** and hiPSC-derived mesenchymal stem cells (iMSCs) induced from iNCCs **(B)**. **(A-a):** Immunocytochemistry on induced NCCs using anti-TFAP2A. Scale bar = 500 μm. **(A-b):** Flow cytometry analysis of iNCCs. Induced NCCs were stained with an anti-CD271, and higher-intensity cells were sorted. **(B-a):** Phase-contrast image of iMSCs. Scale bar = 200 μm. **(B-b):** Flow cytometry analysis of iMSCs. Induced MSCs were stained with anti-CD90, CD73, and CD105 as MSC-positive markers and with an MSC-negative marker cocktail.

general anesthesia, and the study was approved by the Animal Experimentation Committee of Kyoto University.

2.5. Transplantation of C-iMSCs

General anesthesia was induced by an intraperitoneal injection of butorphanol tartrate (0.25 mg/100 g), medetomidine hydrochloride (0.015 mg/100 g), and midazolam (0.2 mg/100 g). Following the separation of bilateral sternohyoid and sternothyroid muscles, thyroid cartilage was separated from the circumferential tissue. After bilateral defects of the thyroid cartilage were created using a biopsy punch (Kai industries, Tokyo, Japan) (outer diameter = 1 mm), preserving the thyroarytenoid muscle, three C-iMSCs were transplanted into defects only the left side. To stabilize the transplanted C-iMSCs, bilateral sternohyoid, and sternothyroid muscles were sutured with 5–0 nylon at one point prior to skin suture. All rats survived the operation, and no complications were observed during the experimental period.

2.6. Histological examination

Following CO_2 euthanasia, the larynx was removed at 4 or 8 weeks postoperatively. The larynx and sternohyoid and sternothyroid muscles were fixed in 4% paraformaldehyde (PFA) in PBS overnight at 4 °C; immersed in 10%, 20%, and 30% sucrose overnight for cryoprotection; and embedded in optimal cutting temperature compound. Axial cryosections were made at a thickness of 10 μm. Hematoxylin and eosin (HE) staining, alcian blue staining, safranin-O staining, and immunohistochemistry (IHC) were conducted using adjacent sections to evaluate cartilage regeneration and engraftment of the transplanted cells. For alcian blue staining, sections were treated with 3% acetic acid for 3 min and stained with Alcian Blue 8GX solution (pH 2.5, 1.061647, Merck KGaA, Darmstadt, Germany) for 30 min. Then, the sections were immersed again in 3% acetic acid for 3 min. The sections were dehydrated and cleared with ethyl alcohol before mounting. The safranin-O staining method was modified from that described in previous reports (Kahveci et al., 2000; Tran et al., 2000). Sections were immersed in Weigert's iron hematoxylin solution for 10 min and stained with 0.05% Fast Green FCF (Sigma-Aldrich, St. Louis, MO, USA) solution for 5 min. Then, the sections were treated with 1% acetic acid. The sections were stained again in 0.1% Safranin-O solution (Sigma-Aldrich) for 5 min, dehydrated, and cleared with ethyl alcohol before mounting.

Sections of C-iMSCs were prepared using the method described

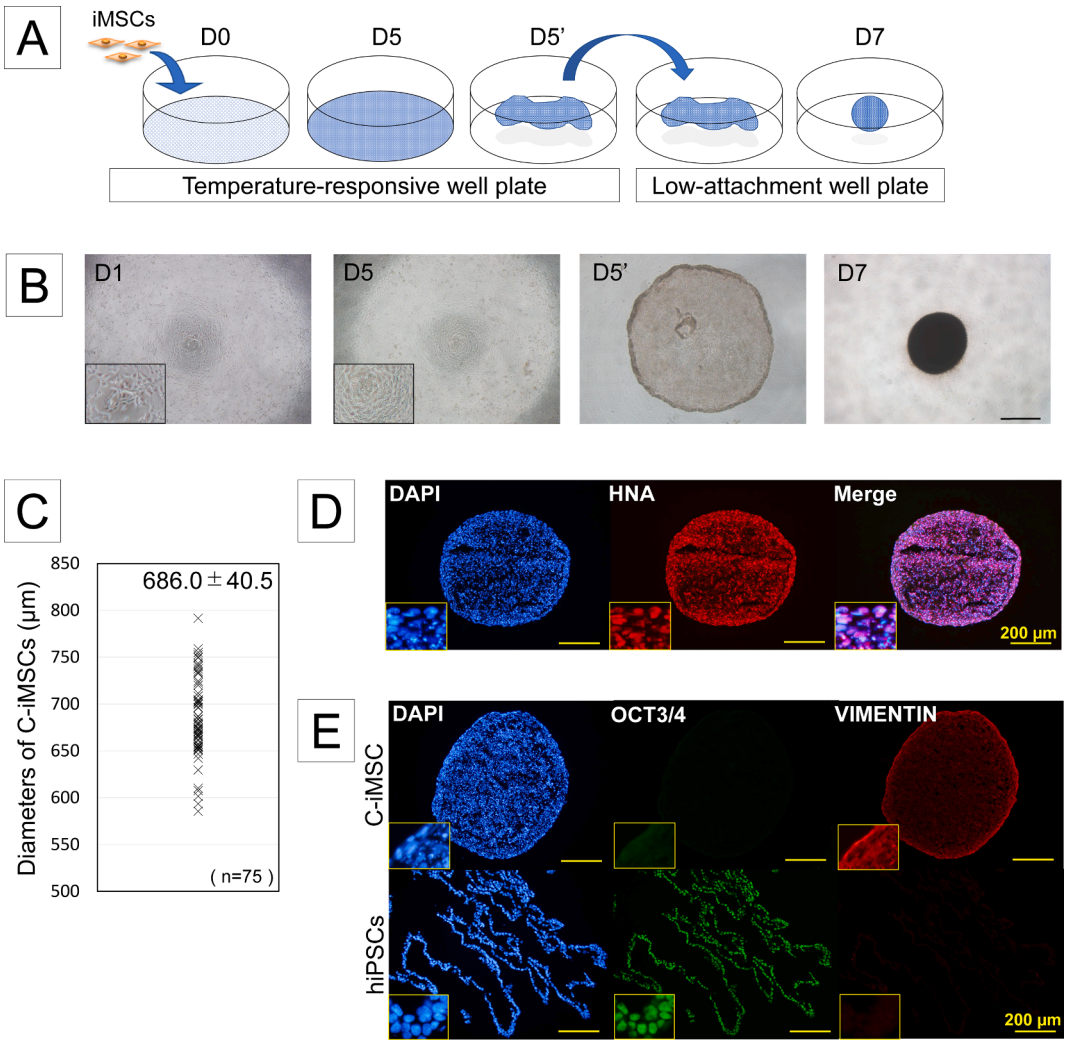

Fig. 2. Fabrication and evaluation of C-iMSCs. **(A):** Schematic protocol for the fabrication of C-iMSCs. Induced MSCs were seeded onto temperature-responsive 96-well plate on Day 0 (D0). On Day 5, after being left to stand at room temperature for 15 min, confluent iMSCs (D5) spontaneously detached as a sheetlike structure (D5′) and were transferred onto a low-attachment 96-well plate. Then, C-iMSCs were obtained on Day 7 (D7). **(B):** Morphology during fabrication of C-iMSC. Phase contrast images from days 1, 5, 5′, and 7. Scale bar = 500 μm. **(C):** Diameters of C-iMSCs (n = 75). **(D):** Immunohistochemistry (IHC) on C-iMSCs with anti-human nuclear antigen (HNA). **(E):** Immunofluorescence staining of sections of C-iMSC and undifferentiated hiPSC sheets with OCT3/4 (green) and VIMENTIN (red). (For interpretation of the references to colour in this figure legend, the reader is referred to the web version of this article.)

above and were used for IHC.

2.7. Immunofluorescence staining of iNCCs

Following fixation with 4% PFA in PBS for 15 min and rinsing with PBS, induced cells were treated with 0.2% Triton X-100 in PBS for 15 min at 4 °C to allow permeabilization. To block nonspecific antibody binding, cells were immersed in Blocking One (Nacalai Tesque, Kyoto, Japan) for 1 h at 4 °C. The cells were then incubated with anti-TFAP2A (Table S1) as a neural crest cell marker and diluted with 10% Blocking One in PBS containing 0.05% Tween 20 (PBST) overnight at 4 °C. The cells were rinsed with PBST and incubated with a fluorophore-labeled secondary antibody (Alexa Fluor-conjugated secondary antibodies, Invitrogen, Tokyo, Japan) and 4‘,6-diamino-2-phenylindole (DAPI; Invitrogen) for nuclei staining for 1 h at room temperature. After further washing with PBS, images were obtained using a fluorescence microscope (Nikon-eclipse Ti-S), Olympus DP73 camera (Olympus), and cellSens Standard software (Olympus).

2.8. Immunofluorescence staining for C-iMSCs and larynx

C-iMSCs sections were treated with 0.2% Triton X-100 in PBS for 5 min at 4 °C to allow permeabilization and immersed in 0.1% BSA/PBS for 10 min at 4 °C to block nonspecific antibody binding. The sections were then incubated overnight at 4 °C with anti-OCT3/4, anti-VIMENTIN, and anti-human nuclear antigen (HNA) antibodies (Table S1) diluted in 0.1% BSA/PBS. The sections were rinsed with PBST and incubated with fluorophore-labeled secondary antibodies and DAPI for 1 h at room temperature. Undifferentiated hiPSC (1231A3) sheets were prepared for OCT3/4-positive control and VIMENTIN-negative control staining. Those sections were simultaneously stained using the same procedure as for C-iMSCs. Signals were visualized using identical exposure times.

For epitope retrieval, larynx sections were digested for 10 min at 37 °C with 0.5% pepsin (Sigma-Aldrich) diluted with 0.5-mM hydrochloric acid for anti-type I collagen and anti-type II collagen antibody reactions. For anti-SOX9 staining, sections were heated in citrate buffer solution (pH 6.0) for 10 min at 98 °C, followed by incubation for additional 30 min at 65 °C. After rinsing with PBS and blocking with Blocking One for 1 h, the sections were incubated overnight at 4 °C with

anti-HNA, anti-type I collagen, anti-type II collagen, and anti-SOX9 antibodies (Table S1). The sections were rinsed with PBST and incubated with fluorophore-labeled secondary antibodies and DAPI for 1 h at room temperature. Antibodies were diluted with Can Get Signal Solution B (Toyobo, Osaka, Japan) for anti-type I collagen and anti-type II collagen staining and with 10% Blocking One in PBST for anti-SOX9 staining. After further washing with PBS, the sections were mounted. All images of sections were obtained using an OLYMPUS BX 50 fluorescence microscope with an Olympus DP70 camera (Olympus), an Olympus DP Controller 2002 (Olympus), and a KEYENCE BZ-9000 fluorescence microscope. Images were analyzed using ImageJ software (2.0.0-rc-68, National Institutes of Health, MD, USA).

3. Results

3.1. Characterization of iNCCs and iMSCs

Immunocytochemistry (ICC) revealed that the obtained NCCs expressed the NCC marker transcription factor activating protein-2α (TFAP2A). After iNCC induction, 62.6% of total cells were sorted with the $CD271^{high}$ population (Fig. 1-A). The presence of fibroblastic cells was evident during the iMSC induction. FACS analysis revealed that iMSC exhibited the surface marker profile of human MSCs (positive for CD90, CD73, and CD105, and negative for CD45, CD34, CD79A, CD11b and HLA-DR) (Fig. 1-B). These findings suggested that induced cells exhibited MSC characteristics. The characterization of iMSCs derived from one hiPSC was confirmed in three independent experiments (Supplementary Fig. S2).

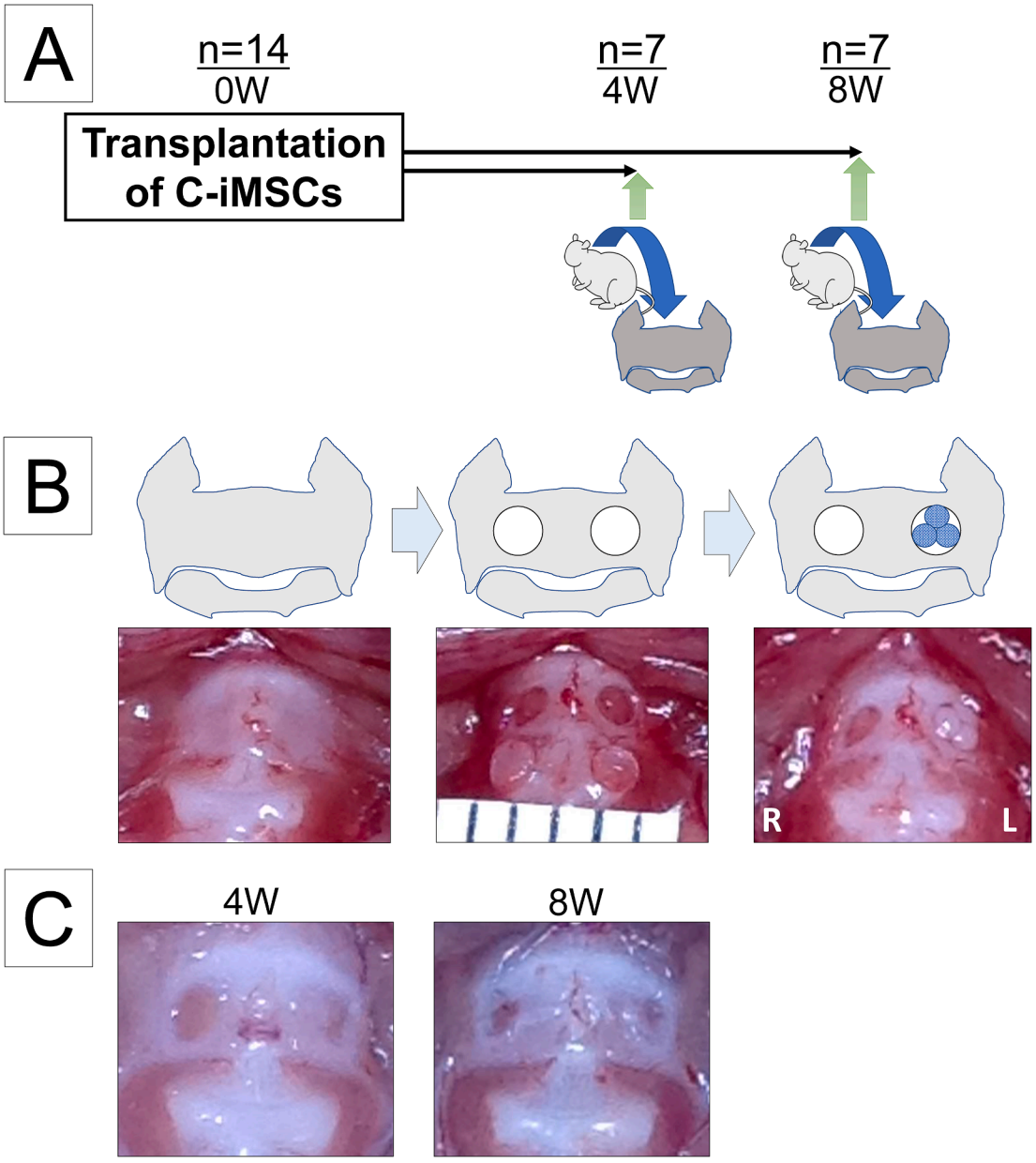

Fig. 3. Transplantation of C-iMSCs and macroscopic findings. **(A):** Schematic protocol for the transplantation of C-iMSCs. Rats were sacrificed at 4 and 8 weeks postoperatively for the histological examination of the larynx. **(B):** Macroscopic images of transplants in thyroid cartilage defects. **(C):** Macroscopic thyroid cartilage findings at 4 and 8 weeks postoperatively.

3.2. Evaluation of C-iMSCs

Seeded iMSCs steadily proliferated, and confluent iMSCs were spontaneously dissociated as a sheetlike structure from temperature-responsive plates on Day 5 after being left to stand at room temperature. Sheetlike structures formed spherical structures on Day 7 after transfer to low-attachment plates (Fig. 2-A, B). The mean diameter of C-iMSCs was 686.0 ± 40.5 μm (Fig. 2-C). Immunofluorescence staining of C-iMSCs revealed HNA expression co-localizing with DAPI (Fig. 2-D). In immunofluorescence staining, C-iMSCs, but not undifferentiated cell sheets, were positive for VIMENTIN, which is a mesenchymal lineage marker. By contrast, C-iMSCs, but not undifferentiated cell sheets, were negative for OCT3/4, which indicates the presence of undifferentiated iPSCs (Fig. 2-E).

3.3. Evaluation of thyroid cartilage regeneration

Three C-iMSCs were transplanted into left thyroid cartilage defects (Fig. 3-A, B). At 4 and 8 weeks postoperatively, macroscopic findings revealed that cartilage defects were partially repaired in the C-iMSC-transplanted defects on the left compared with the untransplanted defects on the right side (Fig. 3-C).

Cartilage-like regenerated tissue with lacunae formation specific to the original cartilage was observed between the sternothyroid and sternohyoid muscles and thyroarytenoid muscle in the transplanted area, but not on the control side on the HE staining (Fig. 4-A). The cartilage-like regenerated tissues were characterized by small lacunae formation and dense cell population compared with the original cartilage. In our preliminary study, C-iMSCs were created and transplanted to thyroid cartilage defects in a few rats individually using three iMSCs that were independently induced from hiPSC through iNCCs. Of these, two iMSCs did not exhibit cartilage-like tissue regeneration by HE staining. Therefore, we selected one iNCC for our experiment. To investigate the reproducibility of the cartilage regeneration ability of iMSCs, three independent inductions of iMSCs derived from one iNCC, fabrication, and transplantation of C-iMSCs were performed. Regeneration of the cartilage-like tissue was observed in three independent induction and transplantation experiments (Supplementary Fig. S1), and in five out of seven rats at 4 and 8 weeks postoperatively (Table 1). Of the 10 rats with cartilage-like regenerated tissue, nine exhibited limited healing of the thyroid cartilage defects (Fig. 5 B-J), except for one rat showed substantial cartilage repair (Fig. 4, Fig. 5-A, and Fig. 6). All cartilage-like regenerated tissues were completely attached to the original thyroid cartilage (Fig. 5).

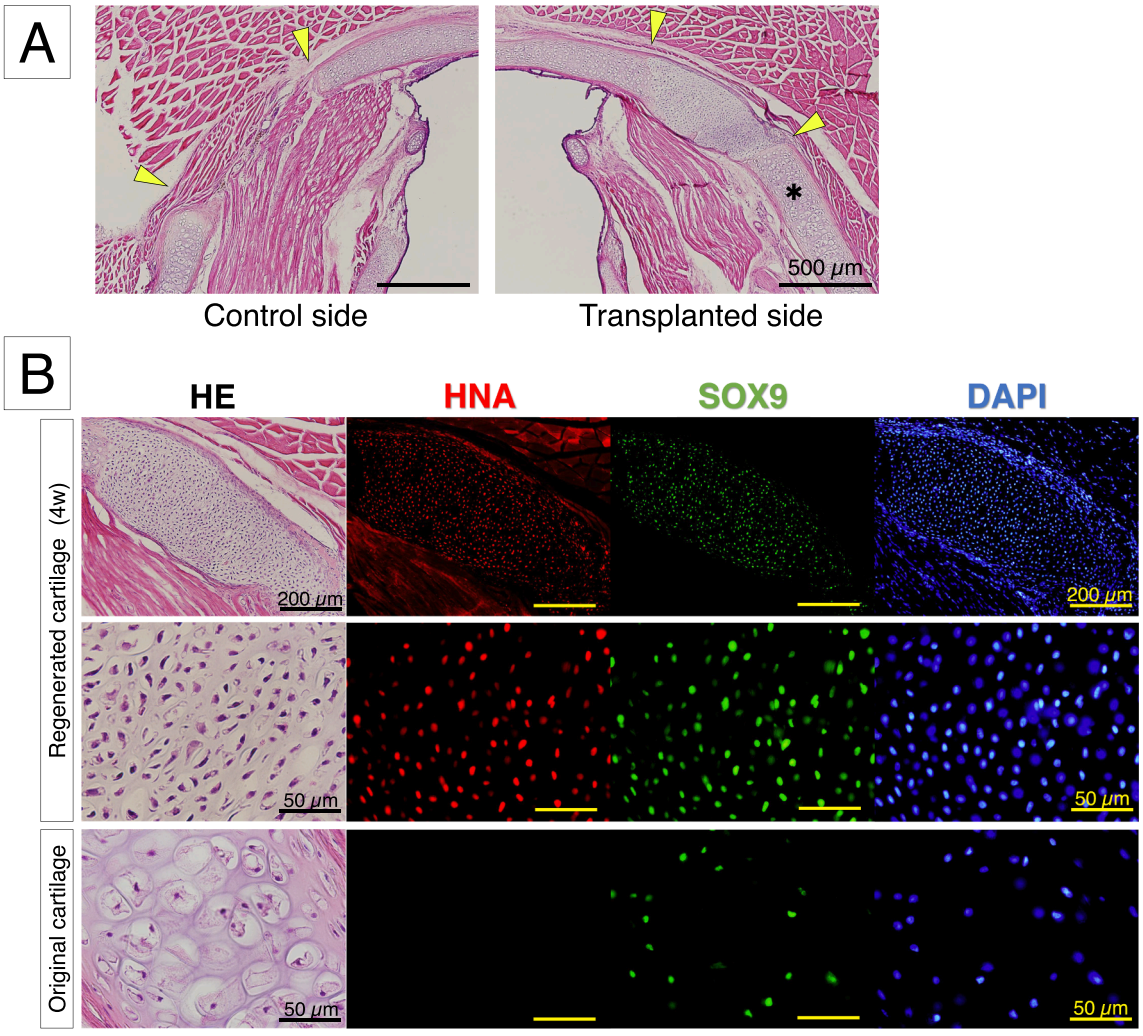

Fig. 4. Histological evaluation of C-iMSC transplanted laryngeal axial sections at 4 weeks postoperatively. **(A):** HE staining of control and transplanted sides. The area between the yellow arrow heads indicates the defect area in the thyroid cartilage. Cartilage-like regenerated tissue was observed in the transplanted area, but not in the control side. **(B):** IHC using anti-HNA (red), anti-SOX9 (green), and DAPI (blue) and HE staining of the cartilage-like regenerated tissue in the C-iMSC-transplanted area compared with the original cartilage (*in Fig. A). (For interpretation of the references to colour in this figure legend, the reader is referred to the web version of this article.)

Table 1
The number of rats confirmed cartilage-like regeneration or HNA-positive cells.

Period	Cartilage-like regeneration (+)	HNA-positive cells (+)
4 W	5 / 7 (71.4%)	7 / 7 (100%)
8 W	5 / 7 (71.4%)	7 / 7 (100%)

The survival of transplanted cells in the area of cartilage-like regeneration was confirmed through HNA immunofluorescence and DAPI staining (for normal nuclear morphology) (Fig. 4-B and Fig. 5). Moreover, HNA-positive cells were observed in both cartilage-like regenerated tissue and fibroblastic cells (Fig. 5-B, D, H, I). In four rats, without cartilage-like regenerated tissue, HNA-positive fibroblastic cells covered the original thyroid cartilage (Supplementary Fig. S3). Thus,

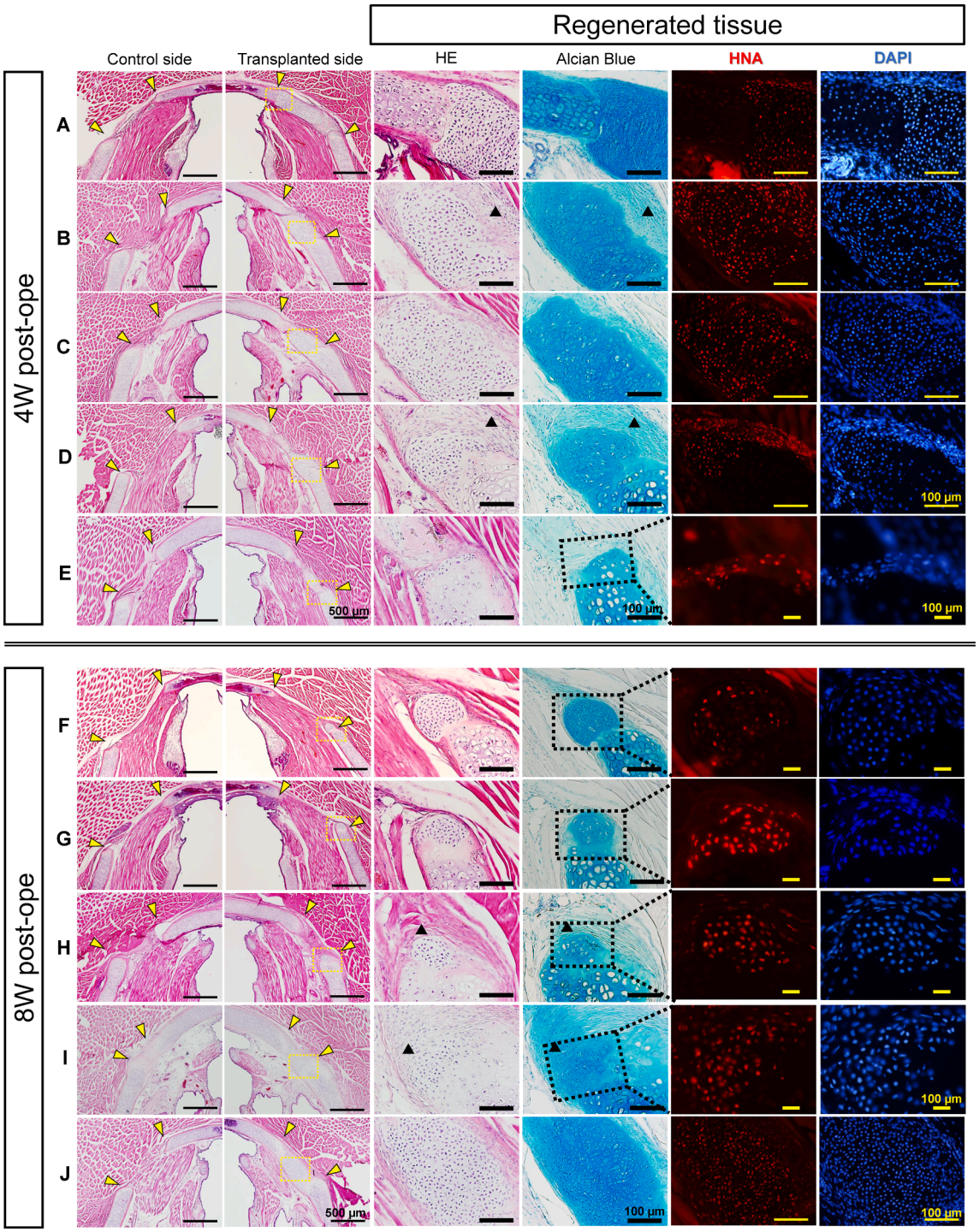

Fig. 5. Histological findings of all rats showed regenerated cartilage-like tissue at 4 (rat A–E) and 8 (rat F–J) weeks postoperatively. The third (HE staining) and fourth columns (alcian blue staining) indicate a higher magnification of the yellow-dotted box in the second column. The fifth and sixth columns indicate IHC, using anti-HNA and DAPI in regenerated tissue, including cartilage-like tissue (rat E–I show higher magnification of black-dotted box in the fourth column). All cartilage-like regenerated tissues were completely attached to the original thyroid cartilage. HNA-positive cells were observed in both cartilage-like regenerated tissue and fibroblastic cells, especially in rats B, D, H, and I (▲). (For interpretation of the references to colour in this figure legend, the reader is referred to the web version of this article.)

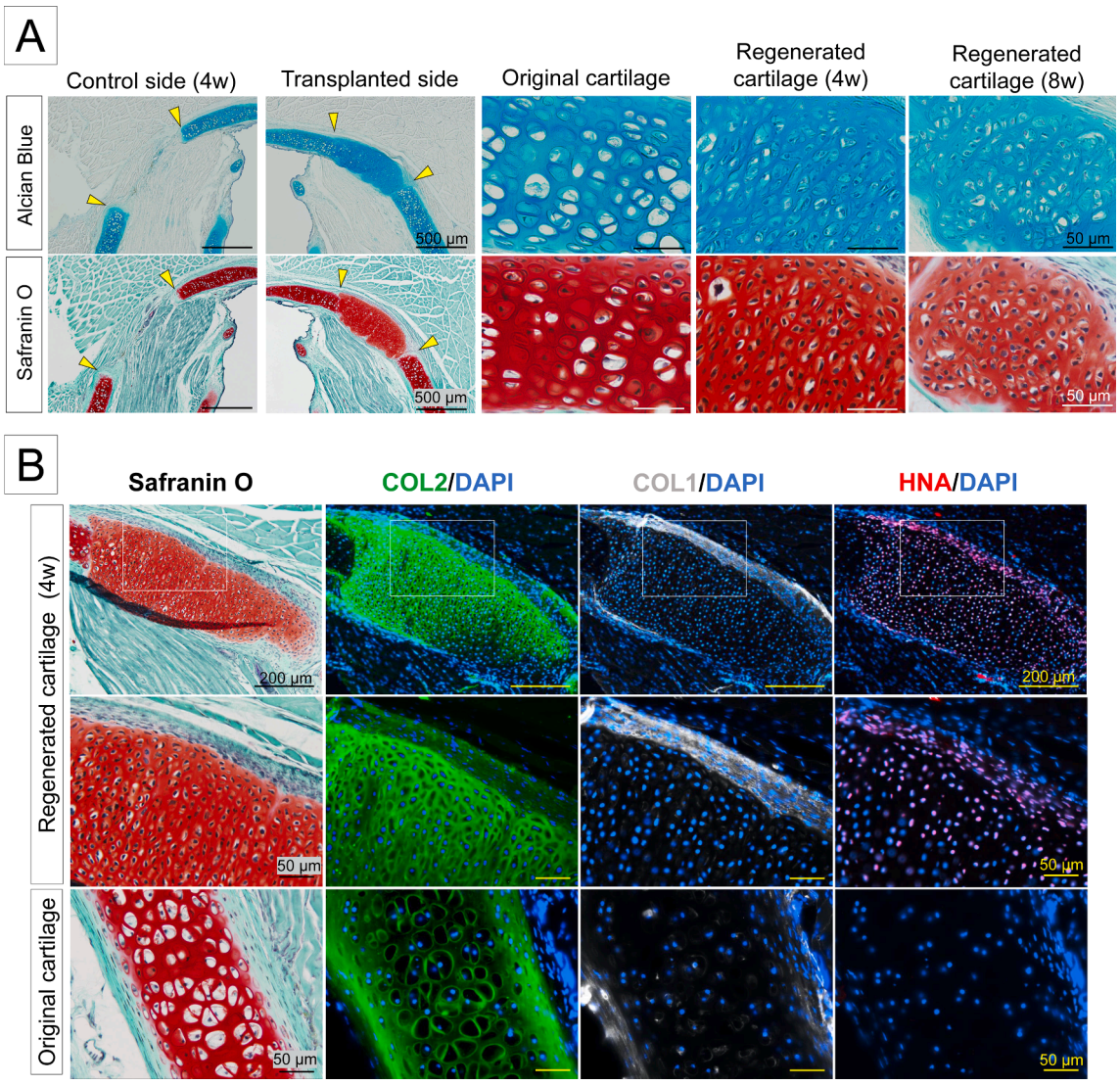

Fig. 6. Evaluation of the extracellular matrix of cartilage-like regenerated tissue. **(A):** Alcian blue and safranin-O staining of the original cartilage and the regenerated area at 4 and 8 weeks postoperatively. **(B):** IHC using anti-type II collagen (green), anti-type I collagen (white), anti-HNA (red) antibody, and DAPI (blue) and safranin-O staining of the regenerated area at 4 weeks postoperatively compared with the original cartilage. Abbreviations: COL1: type I collagen; COL2: type II collagen. (For interpretation of the references to colour in this figure legend, the reader is referred to the web version of this article.)

HNA-positive surviving transplanted cells were observed in all rats at 4 and 8 weeks postoperatively (Table 1), whereas no HNA-positive cells were observed in non-transplanted defects.

In cartilage-like regenerated tissue, almost all HNA-positive cells expressed SOX9, which is a marker of chondroprogenitors and chondrocytes (Yin et al., 2016a) (Fig. 4-B). These findings indicated that transplanted iMSCs partially differentiated into cells with a chondrogenic lineage. By contrast, a few fibroblastic cells around the original thyroid cartilage co-expressed SOX9 in rats that did not exhibit cartilage-like tissue regeneration (Supplementary Fig. S3). These findings were also observed in our preliminary study, where cartilage-like tissue regeneration was not observed (Supplementary Fig. S1 and Fig. S4). We speculated that some surviving transplanted cells tended to differentiate to chondroprogenitor cells without achieving cartilage regeneration.

Analysis of alcian blue and safranin-O staining (used for detecting acidic polysaccharides, such as glycosaminoglycans of the cartilage) revealed extracellular matrix (ECM) staining in the cartilage-like regenerated tissue, which was comparable to that of the original cartilage, but not observed on the control side. No obvious difference was observed in lacunae formation between 4 and 8 weeks postoperatively (Fig. 5 and Fig. 6-A). Type II collagen is an ECM component of the hyaline cartilage; type I collagen is not expressed in the hyaline cartilage but in fibrocartilage and fibrous tissue (Frisbie et al., 1999; Outani et al., 2013). In regenerated tissue with HNA-positive cells, type II collagen was prevalent, whereas type I collagen was absent. Moreover, the surrounding tissue expressed HNA and type I and II collagen (Fig. 6-B).

4. Discussion

In this study, we transplanted iMSCs that we derived from hiPSCs through NCC intermediates into defects in rat thyroid cartilage and confirmed the regeneration of hyaline cartilage-like tissues at the transplanted site without formation of any teratoma. To our knowledge, this is the first study to demonstrate the efficacy, safety, and feasibility of using iMSCs prepared under xeno-free/serum-free conditions for cartilage regeneration *in vivo*. Thus, our results show potential for the application of these cells and methods for hyaline cartilage regeneration in other organs.

Due to their unique properties (proliferative ability; differentiation potency to chondrocytes, adipocytes, osteocytes, etc.; and paracrine effects to promote tissue regeneration and regulate immune reactions

and inflammation (Madrigal et al., 2014; Prockop, 1997; Zhao and Ikeya, 2018), MSCs have been widely used for regenerating osseous or cartilaginous tissues in preclinical and clinical settings (Squillaro et al., 2016). Autologous (Bae et al., 2018; Go Tetsuhiko et al., 2010; Gray et al., 2012), allogeneic (Chang et al., 2014; Ott et al., 2015; Zhang et al., 2018) and human (Ansari et al., 2017; Birchall et al., 2019; Jotz et al., 2014) MSCs combined with artificial materials or decellularized tissues have been used for regenerating laryngotracheal cartilage, and their regenerative potential has been well documented. Based on the promising results in preclinical studies, clinical application of MSCs for laryngotracheal reconstruction has been attempted in combination with decellularized cadaveric homograft. However, restenosis of reconstructed trachea was eventually observed in two out of three patients (Elliott et al., 2017; Hamilton et al., 2015; Molins, 2019), and no reliable treatment option has been established so far.

Owing to their theoretically unlimited proliferative capacity and pluripotency, hiPSCs may be an attractive alternative to autologous or allogeneic MSCs. There has been only one report using hiPSCs for laryngotracheal cartilage regeneration (Kim et al., 2020). In this report, hiPSCs were generated under feeder conditions, and MSCs were induced through embryoid body (EB) formation using fetal bovine serum. They transplanted 3D-printed tubular artificial structures (Polycaprolactone) covered with iMSCs, hiPSC-derived chondrocytes, and human bronchial epithelial cells into rabbit tracheal defects. At 4 weeks postoperatively, cartilage regeneration was observed in the transplanted areas. However, they speculated that cartilage regeneration was not attributable to the differentiation of hiPSC-derived cells, but to cytokines, growth factors, and ECM, because co-expression of HNA and a cartilage surface marker was not observed in the regenerated cartilage. Although the differentiation of iMSCs into cartilaginous lineage cells has not been clearly demonstrated in any organs *in vivo*, we have successfully confirmed the differentiation potential of iMSCs into chondrogenic lineage cells. Transplantation of iMSCs seems to be a promising and feasible strategy for laryngotracheal cartilage regeneration.

Among several iMSC induction methods, the EB formation method (Villa-Diaz et al., 2012) has been well investigated as a classical induction method for cartilage regeneration, with demonstrated cartilaginous regenerative ability (Ko et al., 2014; Rim et al., 2018; Xu et al., 2017; Zhu et al., 2016). Nevertheless, it is possible that the EB formation method leads to heterogeneous cell populations and unpredictable differentiation outcomes because EB formation is generally used for inducing three germ layer cell lineages (Khoo et al., 2005; Nakagawa et al., 2009; Nejadnik et al., 2015). Recently, several researchers have focused on iMSC induction through NCC intermediates (Fukuta et al., 2014; Liu et al., 2012; Menendez et al., 2013), due to homogeneous expansion of NCCs in maintenance culture following purification using anti-CD271 (Fukuta et al., 2014) and ready induction of homogeneous mesenchymal progenitors from iNCCs without additional cell sorting (Chijimatsu et al., 2017). These properties more reliably facilitate the generation of uniform MSCs for transplantation. To date, there has been only one report investigating the efficacy of iMSCs induced from iNCCs on cartilage regeneration *in vivo* (Chijimatsu et al., 2017). However, iMSC induction from iNCCs did not exhibit cartilaginous regenerative ability following transplantation into rat articular defects using sheetlike iMSC structures in this study despite the successful cartilage differentiation *in vitro*. Their pellet culture of iMSCs induced from iNCCs demonstrated serum inhibition of chondrogenesis from iMSCs. Hence, it was suggested that serum or serum-derived factors, which are present in the blood from articular defects, negatively affected cartilage regeneration. In our study, the creation of thyroid cartilage defects also resulted in bleeding. Other factors, including ECM produced by transplanted MSCs or host cartilage, may have influenced cartilage regeneration *in vivo* rather than serum.

Various reports have demonstrated that MSC-derived ECM promoted chondrogenic differentiation and cartilage regeneration (Zhang et al., 2016). Initially, cartilage development initiates mesenchymal condensation (DeLise et al., 2000). Three-dimensional culture systems, including pellet culture and micromass culture, have been widely used for chondrogenic differentiation of MSCs *in vitro* (Zhang et al., 2010). Kittaka et al. revealed that the clump-forming three-dimensional culture system encouraged abundant ECM production by rat MSCs (Kittaka et al., 2015). Thus, it was suggested that C-iMSC-derived ECM promoted cartilaginous differentiation of iMSCs, unlike sheetlike structures (Chijimatsu et al., 2017).

Host-derived cartilage-ECM have also been reported to promote chondrogenic differentiation of stem cells (Yin et al., 2016b). In our study, all cartilage-like regenerated tissues were intimately attached to the original rat thyroid cartilage. Therefore, we speculate that the host cartilage-ECM might affect the cartilage differentiation of transplanted iMSCs.

Our histological results revealed a variation in the area of cartilage regeneration in each case using iMSCs derived from one iNCC. Additionally, two out of three iMSCs derived from iNCCs in three independent experiments showed HNA-positive surviving cells, co-expressing SOX9, but no cartilage regeneration (Supplementary Fig. S1 and Fig. S4), despite proper induction of iMSCs (Supplementary Fig. S2). These results may have been affected by two factors. First, induction from iPSCs causes variations in induction efficiency and the viability and differentiation capacity of induced cells, even under same culture conditions. To confirm the robustness and improve reproducibility of our experimental protocol, modification in the induction protocol for generating iMSCs through NCC intermediates and selection of iPSC lines suitable for cartilage regeneration are required. Moreover, the size of C-iMSCs fabricated from the same iNCC varied before transplantation (Fig. 2-C). Therefore, modification in C-iMSC fabrication method, including that of culture systems, periods of culture, and cell density, may improve cell viability, survival rate, and cartilage regeneration. Second, immune reactions to xenotransplantation inevitably affect engraftment efficiency and may have caused variability in our results. X-SCID rats were utilized to avoid immune rejection by the host; however, the immune systems of these rats are not completely depleted (Mashimo et al., 2010). It is known that human MSCs have immunomodulatory properties (Madrigal et al., 2014), and it has been demonstrated that iMSCs induced from iNCCs also have immunomodulatory properties under xenogeneic conditions (Mitsuzawa et al., 2019). Allogeneic MSC transplantation has been widely used in clinical settings, and HLA-editing techniques may provide safety and feasibility in using hiPSCs for allogeneic transplantation (Xu et al., 2019). Allogeneic iMSC transplantation may lead to more effective cartilage regeneration than xenogeneic transplantation.

The present study has some limitations, including relatively short periods for histological analysis following transplantation. Also, biomechanical strength was not elucidated for regenerated cartilage-like tissue. In this study, periods of 4 and 8 weeks after operation were selected according to previous studies (Chang et al., 2014; Chijimatsu et al., 2017). Our histological examinations demonstrated the formation of smaller lacunae in the transplanted site than in the original cartilage; however, there was no obvious difference observed between these two periods. In general, chondrocytes begin producing ECM and adopt a rounded morphology encased within that ECM during chondrogenic differentiation from mesenchymal cells. Therefore, hypertrophy occurs during further differentiation (DeLise et al., 2000). Longer periods may contribute to maturation during cartilage-like tissue regeneration and provide information about chondrogenic differentiation and long-term survival of HNA and SOX9 positive cells without cartilage-like tissue regeneration. In the clinical setting, tubular structure retention is indispensable for airway function. Transplanted materials require tolerance for external and respiratory pressures over a long period of time. Larger transplant size in a larger animal model and longer periods of observation are needed to support application of this in humans. We plan to create large transplants comprising multiple C-iMSCs using a bio-three-dimensional printer (Mitsuzawa et al., 2020; Yurie et al., 2017) to

examine their strength and compression tolerance.

5. Conclusion

We investigated the efficacy of iMSCs in the regeneration of thyroid cartilage in a rat model. Moreover, we induced iMSCs differentiated through NCC intermediates under xeno-free/serum-free conditions to evaluate their potential for clinical application and confirmed the expression of specific NCC and MSC markers. In vivo studies using C-iMSCs revealed that C-iMSCs encouraged cartilage regeneration and that some of the surviving iMSCs differentiated into chondrogenic lineage cells in thyroid cartilage defects in immunodeficient rats post-operatively. Our results suggest that iMSCs as a candidate technology for human laryngotracheal reconstruction.

Declaration of Competing Interest

The authors declare that they have no known competing financial interests or personal relationships that could have appeared to influence the work reported in this paper.

Acknowledgements

We thank the Center for Anatomical, Pathological and Forensic Medical Research, Kyoto University Graduate School of Medicine, for preparing microscope slides (safranin-O staining sections), Dr. Daisuke Kamiya for the advice of C-iMSC generation, and Dr. Naoki Yamada for the advice of iNCC induction. Flow cytometry analyses using BD FACS Aria II and BD LSRFortessa Cell Analyzer were performed at the Medical Research Support Center, Graduate School of Medicine, Kyoto University, which was supported by Platform for Drug Discovery, Informatics, and Structural Life Science from the Ministry of Education, Culture, Sports, Science and Technology, Japan.

Funding

This work was supported in part by the Grant-in-Aid for Early-Career Scientists from Japan Society for the Promotion of Science (19 K18803) and alumni otolaryngology fund from the Department of Otolaryngology Head and Neck Surgery, Graduate School of Medicine, Kyoto University.

Appendix A. Supplementary data

Supplementary data to this article can be found online at https://doi.org/10.1016/j.scr.2021.102233.

References

Akiyama, Y., Kikuchi, A., Yamato, M., Okano, T., 2014. Accelerated cell-sheet recovery from a surface successively grafted with polyacrylamide and poly(N-isopropylacrylamide). Acta Biomater. 10 (8), 3398–3408. https://doi.org/10.1016/j.actbio.2014.03.024.

Albrecht, N.M., Ostrower, S., 2019. Case report of a laryngotracheal reconstruction with anterior and posterior costal cartilage graft and stent placement – Surgical technique. Int. J. Surgery Case Rep. 58, 145–152. https://doi.org/10.1016/j.ijscr.2019.04.009.

Ansari, T., Lange, P., Southgate, A., Greco, K., Carvalho, C., Partington, L., Bullock, A., MacNeil, S., Lowdell, M.W., Sibbons, P.D., Birchall, M.A., 2017. Stem Cell-Based Tissue-Engineered Laryngeal Replacement: Tissue-Engineered Laryngeal Replacement. STEM CELLS Transl. Med. 6 (2), 677–687. https://doi.org/10.5966/sctm.2016-0130.

Astori, G., Amati, E., Bambi, F., Bernardi, M., Chieregato, K., Schäfer, R., Sella, S., Rodeghiero, F., 2016. Platelet lysate as a substitute for animal serum for the ex-vivo expansion of mesenchymal stem/stromal cells: present and future. Stem Cell Res. Ther. 7 (1) https://doi.org/10.1186/s13287-016-0352-x.

Bae, S.-W., Lee, K.-W., Park, J.-H., Lee, J., Jung, C.-R., Yu, J., Kim, H.-Y., Kim, D.-H., 2018. 3D Bioprinted Artificial Trachea with Epithelial Cells and Chondrogenic-Differentiated Bone Marrow-Derived Mesenchymal Stem Cells. Int. J. Mol. Sci. 19, 1624. Doi: 10.3390/ijms19061624.

Bhosale, A.M., Richardson, J.B., 2008. Articular cartilage: structure, injuries and review of management. Br. Med. Bull. 87, 77–95. Doi: 10.1093/bmb/ldn025.

Birchall, M.A., Herrmann, P., Sibbons, P., Birchall, M., 2019. In vivo feasibility study of the use of porous polyhedral oligomeric silsesquioxane implants in partial laryngeal reconstruction. bioRxiv 587691. Doi: 10.1101/587691.

Chang, E., Wu, L., Masters, J., Lu, J., Zhou, S., Zhao, W., Sun, M., Meng, F., Soo, C.P., Zhang, J., Ma, D., 2019. Iatrogenic subglottic tracheal stenosis after tracheostomy and endotracheal intubation: A cohort observational study of more severity in keloid phenotype. Acta Anaesthesiol Scand 63 (7), 905–912. https://doi.org/10.1111/aas.13371.

Chang, J.W., Park, S.A., Park, J.-K., Choi, J.W., Kim, Y.-S., Shin, Y.S., Kim, C.-H., 2014. Tissue-Engineered Tracheal Reconstruction Using Three-Dimensionally Printed Artificial Tracheal Graft: Preliminary Report: Tracheal Reconstruction with 3D-Printed Graft. Artif. Organs 38 (6), E95–E105. https://doi.org/10.1111/aor.12310.

Chiang, T., Pepper, V., Best, C., Onwuka, E., Breuer, C.K., Author, C., Otol Rhinol Laryngol Author manuscript, A., 2016. Clinical Translation of Tissue Engineered Trachea Grafts HHS Public Access Author manuscript. Ann Otol. Rhinol. Laryngol. 125, 873–885. Doi: 10.1177/0003489416656646.

Chijimatsu, Ryota, Ikeya, Makoto, Yasui, Yukihiko, Ikeda, Yasutoshi, Ebina, Kosuke, Moriguchi, Yu, Shimomura, Kazunori, Hart, David A, Yoshikawa, Hideki, Nakamura, Norimasa, 2017. Characterization of Mesenchymal Stem Cell-Like Cells Derived From Human iPSCs via Neural Crest Development and Their Application for Osteochondral Repair. Stem Cells Int. 2017, 1–18. https://doi.org/10.1155/2017/1960965.

Pauken, Christine M., Heyes, Richard, Lott, David G., 2019. Mechanical, Cellular, and Proteomic Properties of Laryngotracheal Cartilage. CARTILAGE 10 (3), 321–328. https://doi.org/10.1177/1947603517749921.

de Sousa, P.A., Galea, G., Turner, M., 2006. The road to providing human embryo stem cells for therapeutic use: The UK experience. Reproduction 132, 681–689. Doi: 10.1530/rep.1.01080.

DeLise, A.M., Fischer, L., Tuan, R.S., 2000. Cellular interactions and signaling in cartilage development. Osteoarth. Cartil. 8 (5), 309–334. https://doi.org/10.1053/joca.1999.0306.

Elliott, Martin J., Butler, Colin R., Varanou-Jenkins, Aikaterini, Partington, Leanne, Carvalho, Carla, Samuel, Edward, Crowley, Claire, Lange, Peggy, Hamilton, Nicholas J., Hynds, Robert E., Ansari, Tahera, Sibbons, Paul, Fierens, Anja, McLaren, Claire, Roebuck, Derek, Wallis, Colin, Muthialu, Nagarajan, Hewitt, Richard, Crabbe, David, Janes, Sam M., De Coppi, Paolo, Lowdell, Mark W., Birchall, Martin A., 2017. Tracheal Replacement Therapy with a Stem Cell-Seeded Graft: Lessons from Compassionate Use Application of a GMP-Compliant Tissue-Engineered Medicine: GMP Production of Tissue-Engineered Trachea. STEM CELLS Transl. Med. 6 (6), 1458–1464. https://doi.org/10.1002/sctm.16-0443.

Frisbie, D.D., Trotter, G.W., Powers, B.E., Rodkey, W.G., Steadman, J.R., Howard, R.D., Park, R.D., McIlwraith, C.W., 1999. Arthroscopic subchondral bone plate microfracture technique augments healing of large chondral defects in the radial carpal bone and medial femoral condyle of horses. Veterinary Surgery 28, 242–255. Doi: 10.1053/jvet.1999.0242.

Fukuta, M., Nakai, Y., Kirino, K., Nakagawa, M., Sekiguchi, K., 2014. Derivation of Mesenchymal Stromal Cells from Pluripotent Stem Cells through a Neural Crest Lineage using Small Molecule Compounds with Defined Media. PLoS ONE 9, 112291. https://doi.org/10.1371/journal.pone.

Go, Tetsuhiko, Jungebluth, Philipp, Baiguero, Silvia, Asnaghi, Adelaide, Martorell, Jaume, Ostertag, Helmut, Mantero, Sara, Birchall, Martin, Bader, Augustinus, Macchiarini, Paolo, 2010. Both epithelial cells and mesenchymal stem cell–derived chondrocytes contribute to the survival of tissue-engineered airway transplants in pigs. J. Thora. Cardiovasc. Surg. 139 (2), 437–443. https://doi.org/10.1016/j.jtcvs.2009.10.002.

Gray, Fabienne L., Turner, Christopher G., Ahmed, Azra, Calvert, Catherine E., Zurakowski, David, Fauza, Dario O., 2012. Prenatal tracheal reconstruction with a hybrid amniotic mesenchymal stem cells–engineered construct derived from decellularized airway. J. Pediatr. Surg. 47 (6), 1072–1079. https://doi.org/10.1016/j.jpedsurg.2012.03.006.

Hamilton, N.J., Kanani, M., Roebuck, D.J., Hewitt, R.J., Cetto, R., Culme-Seymour, E.J., Toll, E., Bates, A.J., Comerford, A.P., McLaren, C.A., Butler, C.R., Crowley, C., McIntyre, D., Sebire, N.J., Janes, S.M., O'Callaghan, C., Mason, C., de Coppi, P., Lowdell, M.W., Elliott, M.J., Birchall, M.A., 2015. Tissue-Engineered Tracheal Replacement in a Child: A 4-Year Follow-Up Study. Am. J. Transplant. 15, 2750–2757. Doi: 10.1111/ajt.13318.

Hashimoto, Yusuke, Nishida, Yohei, Takahashi, Shinji, Nakamura, Hiroaki, Mera, Hisashi, Kashiwa, Kaori, Yoshiya, Shinichi, Inagaki, Yusuke, Uematsu, Kota, Tanaka, Yasuhito, Asada, Shigeki, Akagi, Masao, Fukuda, Kanji, Hosokawa, Yoshiya, Myoui, Akira, Kamei, Naosuke, Ishikawa, Masakazu, Adachi, Nobuo, Ochi, Mitsuo, Wakitani, Shigeyuki, 2019. Transplantation of autologous bone marrow-derived mesenchymal stem cells under arthroscopic surgery with microfracture versus microfracture alone for articular cartilage lesions in the knee: A multicenter prospective randomized control clinical trial. Regenerative Therapy 11, 106–113. https://doi.org/10.1016/j.reth.2019.06.002.

Im, Gun-Il, Shin, Yong-Woon, Lee, Kee-Byung, 2005. Do adipose tissue-derived mesenchymal stem cells have the same osteogenic and chondrogenic potential as bone marrow-derived cells? Osteoarthr. Cartil. 13 (10), 845–853. https://doi.org/10.1016/j.joca.2005.05.005.

Jotz, G.P., da Luz Soster, P.R., Kunrath, S.O., Steffens, D., Braghirolli, D.I., Zettler, C.G., Beck, C.A., Muccillo, M., Lopes, R.F.F., Mastella, B., Pranke, P., 2014. Mesenchymal stem cells and nanofibers as scaffolds for the regeneration of thyroid cartilage. The Laryngoscope 124, E455–E460. Doi: 10.1002/lary.24805.

Kahveci, Zeynep, Minbay, F. Zehra, Cavusoglu, Ilkin, 2000. Safranin O Staining Using a Microwave Oven. Biotech. Histochem. 75 (6), 264–268. https://doi.org/10.3109/10520290009085130.

Kamiya, D., Takenaka-Ninagawa, N., Motoike, S., Kajiya, M., Akaboshi, T., Zhao, C., Shibata, M., Senda, S., Toyooka, Y., Sakurai, H., Kurihara, H., Ikeya, M., 2020, Unpublished results. Induction of Functional Mesenchymal Stem/Stromal Cells from Human iPCs Via a Neural Crest Cell Lineage Under Xeno-Free Conditions. SSRN Electronic J. Doi: 10.2139/ssrn.3741231.

Khoo, M.L.M., McQuade, L.R., Smith, M.S.R., Lees, J.G., Sidhu, K.S., Tuch, B.E., 2005. Growth and Differentiation of Embryoid Bodies Derived from Human Embryonic Stem Cells: Effect of Glucose and Basic Fibroblast Growth Factor1. Biol. Reproduct. 73, 1147–1156. Doi: 10.1095/biolreprod.104.036673.

Kim, I.G., Park, S.A., Lee, S.H., Choi, J.S., Cho, H., Lee, S.J., Kwon, Y.W., Kwon, S.K., 2020. Transplantation of a 3D-printed tracheal graft combined with iPS cell-derived MSCs and chondrocytes. Sci. Rep. 10, 1–14. https://doi.org/10.1038/s41598-020-61405-4.

Kittaka, M., Kajiya, M., Shiba, H., Takewaki, M., Takeshita, K., Khung, R., Fujita, Takako, Iwata, T., Nguyen, T.Q., Ouhara, K., Takeda, K., Fujita, Tsuyoshi, Kurihara, H., 2015. Clumps of a mesenchymal stromal cell/extracellular matrix complex can be a novel tissue engineering therapy for bone regeneration. Cytotherapy 17, 860–873. https://doi.org/10.1016/j.jcyt.2015.01.007.

Ko, J.Y., Kim, K. il, Park, S., Im, G. il, 2014. In vitro chondrogenesis and in vivo repair of osteochondral defect with human induced pluripotent stem cells. Biomaterials 35, 3571–3581. Doi: 10.1016/j.biomaterials.2014.01.009.

Kretlow, James D, Jin, Yu-Qing, Liu, Wei, Zhang, Wen, Hong, Tan-Hui, Zhou, Guangdong, Baggett, L Scott, Mikos, Antonios G, Cao, Yilin, 2008. Donor age and cell passage affects differentiation potential of murine bone marrow-derived stem cells. BMC Cell Biol. 9 (1), 60. https://doi.org/10.1186/1471-2121-9-60.

La Noce, Marcella, Paino, Francesca, Spina, Anna, Naddeo, Pasqualina, Montella, Roberta, Desiderio, Vincenzo, De Rosa, Alfredo, Papaccio, Gianpaolo, Tirino, Virginia, Laino, Luigi, 2014. Dental pulp stem cells: State of the art and suggestions for a true translation of research into therapy. J. Dent. 42 (7), 761–768. https://doi.org/10.1016/j.jdent.2014.02.018.

Liu, Q., Spusta, S.C., Mi, R., Lassiter, R.N.T., Stark, M.R., Höke, A., Rao, M.S., Zeng, X., 2012. Human Neural Crest Stem Cells Derived from Human ESCs and Induced Pluripotent Stem Cells: Induction, Maintenance, and Differentiation into Functional Schwann Cells. STEM CELLS Transl. Med. 1, 266–278. Doi: 10.5966/sctm.2011-0042.

Ma, B., Leijten, J.C.H., Wu, L., Kip, M., van Blitterswijk, C.A., Post, J.N., Karprien, M., 2013. Gene expression profiling of dedifferentiated human articular chondrocytes in monolayer culture. Osteoarthr. Cartil. 21, 599–603. https://doi.org/10.1016/j.joca.2013.01.014.

Madrigal, Marialaura, Rao, Kosagisharaf S, Riordan, Neil H, 2014. A review of therapeutic effects of mesenchymal stem cell secretions and induction of secretory modification by different culture methods. J. Transl. Med. 12 (1) https://doi.org/10.1186/s12967-014-0260-8.

Mashimo, T., Takizawa, A., Voigt, B., Yoshimi, K., Hiai, H., Kuramoto, T., Serikawa, T., 2010. Generation of knockout rats with X-linked severe combined immunodeficiency (X-SCID) using zinc-finger nucleases. PLoS ONE 5. Doi: 10.1371/journal.pone.0008870.

Menendez, Laura, Kulik, Michael J, Page, Austin T, Park, Sarah S, Lauderdale, James D, Cunningham, Michael L, Dalton, Stephen, 2013. Directed differentiation of human pluripotent cells to neural crest stem cells. Nat. Protoc. 8 (1), 203–212. https://doi.org/10.1038/nprot.2012.156.

Mitsuzawa, Sadaki, Ikeguchi, Ryosuke, Aoyama, Tomoki, Ando, Maki, Takeuchi, Hisataka, Yurie, Hirofumi, Oda, Hiroki, Noguchi, Takashi, Ohta, Souichi, Zhao, Chengzhu, Ikeya, Makoto, Matsuda, Shuichi, 2019. Induced pluripotent stem cell-derived mesenchymal stem cells prolong hind limb survival in a rat vascularized composite allotransplantation model. Microsurgery 39 (8), 737–747. https://doi.org/10.1002/micr.30507.

Mitsuzawa, Sadaki, Zhao, Chengzhu, Ikeguchi, Ryosuke, Aoyama, Tomoki, Kamiya, Daisuke, Ando, Maki, Takeuchi, Hisataka, Akieda, Shizuka, Nakayama, Koichi, Matsuda, Shuichi, Ikeya, Makoto, 2020. Pro-angiogenic scaffold-free Bio three-dimensional conduit developed from human induced pluripotent stem cell-derived mesenchymal stem cells promotes peripheral nerve regeneration. Sci. Rep. 10 (1) https://doi.org/10.1038/s41598-020-68745-1.

Molins, Laureano, 2019. Patient follow-up after tissue-engineered airway transplantation. The Lancet 393 (10176), 1099. https://doi.org/10.1016/S0140-6736(19)30485-4.

Na, Yuyan, Shi, Yuting, Liu, Wanlin, Jia, Yanbo, Kong, Lingyue, Zhang, Ting, Han, Changxu, Ren, Yizhong, 2019. Is implantation of autologous chondrocytes superior to microfracture for articular-cartilage defects of the knee? A systematic review of 5-year follow-up data. Int. J. Surg. 68, 56–62. https://doi.org/10.1016/j.ijsu.2019.06.007.

Nakagawa, Masato, Taniguchi, Yukimasa, Senda, Sho, Takizawa, Nanako, Ichisaka, Tomoko, Asano, Kanako, Morizane, Asuka, Doi, Daisuke, Takahashi, Jun, Nishizawa, Masatoshi, Yoshida, Yoshinori, Toyoda, Taro, Osafune, Kenji, Sekiguchi, Kiyotoshi, Yamanaka, Shinya, 2014. A novel efficient feeder-free culture system for the derivation of human induced pluripotent stem cells. Sci. Rep. 4 (1) https://doi.org/10.1038/srep03594.

Nakagawa, T., Lee, S.Y., Reddi, A.H., 2009. Induction of chondrogenesis from human embryonic stem cells without embryoid body formation by bone morphogenetic protein 7 and transforming growth factor β1. Arthritis Rheum. 60, 3686–3692. https://doi.org/10.1002/art.27229.

Nejadnik, H., Diecke, S., Lenkov, O.D., Chapelin, F., Donig, J., Tong, X., Derugin, N., Chan, R.C.F., Gaur, A., Yang, F., Wu, J.C., Daldrup-Link, H.E., 2015. Improved Approach for Chondrogenic Differentiation of Human Induced Pluripotent Stem Cells. Stem cell Rev. Rep. 11, 242–253. Doi: 10.1007/s12015-014-9581-5.

Nejadnik, Hossein, Hui, James H., Feng Choong, Erica Pei, Tai, Bee-Choo, Lee, Eng Hin, 2010. Autologous Bone Marrow–Derived Mesenchymal Stem Cells Versus Autologous Chondrocyte Implantation: An Observational Cohort Study. Am. J. Sports Med. 38 (6), 1110–1116. https://doi.org/10.1177/0363546509359067.

Ott, Lindsey M., Vu, Cindy H., Farris, Ashley L., Fox, Katrina D., Galbraith, Richard A., Weiss, Mark L., Weatherly, Robert A., Detamore, Michael S., 2015. Functional Reconstruction of Tracheal Defects by Protein-Loaded, Cell-Seeded, Fibrous Constructs in Rabbits. Tissue Eng. Part A 21 (17-18), 2390–2403. https://doi.org/10.1089/ten.tea.2015.0157.

Outani, H., Okada, M., Yamashita, A., Nakagawa, K., Yoshikawa, H., 2013. Direct Induction of Chondrogenic Cells from Human Dermal Fibroblast Culture by Defined Factors. PLoS ONE 8, 77365. Doi: 10.1371/journal.pone.0077365.

Prockop, Darwin J., 1997. Marrow Stromal Cells as Stem Cells for Nonhematopoietic Tissues. Science 276 (5309), 71–74. https://doi.org/10.1126/science:276.5309.71.

Rim, Yeri Alice, Nam, Yoojun, Park, Narae, Lee, Jennifer, Park, Sung-hwan, Ju, Ji Hyeon, 2018. Repair potential of nonsurgically delivered induced pluripotent stem cell-derived chondrocytes in a rat osteochondral defect model. J. Tissue Eng. Regen. Med. 12 (8), 1843–1855. https://doi.org/10.1002/term.2705.

Squillaro, Tiziana, Peluso, Gianfranco, Galderisi, Umberto, 2016. Clinical Trials with Mesenchymal Stem Cells: An Update. Cell Transplant 25 (5), 829–848. https://doi.org/10.3727/096368915X689622.

Tabler, J.M., Rigney, M.M., Berman, G.J., Gopalakrishnan, S., Heude, E., Al-Lami, H.A., Yannakoudiadkis, B.Z., Fitch, R.D., Carter, C., Vokes, S., Liu, K.J., Tajbakhsh, S., Egnor, S.E.R., Wallingford, J.B., 2017. Cilia-mediated hedgehog signaling controls form and function in the mammalian larynx. eLife 6. Doi: 10.7554/eLife.19153.

Tran, D., Golick, M., Rabinovitz, H.S., Rivlin, D., Elgart, G., Nordlow, B., 2000. Hematoxylin and safranin O staining of frozen sections. Dermatologic Surgery 26, 197–199. Doi: 10.1046/j.1524-4725.2000.09220.x.

Uto, Sakura, Nishizawa, Satoru, Hikita, Atsuhiko, Takato, Tsuyoshi, Hoshi, Kazuto, 2018. Application of induced pluripotent stem cells for cartilage regeneration in CLAWN miniature pig osteochondral replacement model. Regenerat. Therapy 9, 58–70. https://doi.org/10.1016/j.reth.2018.06.003.

Villa-Diaz, L.G., Brown, S.E., Liu, Y., Ross, A.M., Lahann, J., Parent, J.M., Krebsbach, P. H., 2012. Derivation of Mesenchymal Stem Cells from Human Induced Pluripotent Stem Cells Cultured on Synthetic Substrates. STEM CELLS 30 (6), 1174–1181. https://doi.org/10.1002/stem.1084.

von der Mark, K., Gauss, V., von der Mark, H., Müller, P., 1971. Relationship between cell shape and type of collagen synthesised as chondrocytes lose their cartilage phenotype in culture. J. R. & Swoveland. P. New Engl. J. Med 173, 397–399.

Wagner, W., Horn, P., Castoldi, M., Diehlmann, A., Bork, S., 2008. Replicative Senescence of Mesenchymal Stem Cells: A Continuous and Organized Process. PLoS ONE 3, 2213. Doi: 10.1371/journal.pone.0002213.

Wakitani, Shigeyuki, Okabe, Takahiro, Horibe, Shuji, Mitsuoka, Tomoki, Saito, Masanobu, Koyama, Tsuyoshi, Nawata, Masashi, Tensho, Keiji, Kato, Hiroyuki, Uematsu, Kota, Kuroda, Ryosuke, Kurosaka, Masahiro, Yoshiya, Shinichi, Hattori, Koji, Ohgushi, Hajime, 2011. Safety of autologous bone marrow-derived mesenchymal stem cell transplantation for cartilage repair in 41 patients with 45 joints followed for up to 11 years and 5 months. J. Tissue Eng. Regen. Med. 5 (2), 146–150. https://doi.org/10.1002/term.299.

Xu, Huaigeng, Wang, Bo, Ono, Miyuki, Kagita, Akihiro, Fujii, Kaho, Sasakawa, Noriko, Ueda, Tatsuki, Gee, Peter, Nishikawa, Misato, Nomura, Masaki, Kitaoka, Fumiyo, Takahashi, Tomoko, Okita, Keisuke, Yoshida, Yoshinori, Kaneko, Shin, Hotta, Akitsu, 2019. Targeted Disruption of HLA Genes via CRISPR-Cas9 Generates iPSCs with Enhanced Immune Compatibility. Cell Stem Cell 24 (4), 566–578.e7. https://doi.org/10.1016/j.stem.2019.02.005.

Xu, X., Shi, D., Liu, Y., Yao, Y., Dai, J., Xu, Z., Chen, D., Teng, H., Jiang, Q., 2017. In vivo repair of full-thickness cartilage defect with human iPSC-derived mesenchymal progenitor cells in a rabbit model. Exp. Therapeut. Med. 14, 239–245. Doi: 10.3892/etm.2017.4474.

Yamashita, Akihiro, Morioka, Miho, Yahara, Yasuhito, Okada, Minoru, Kobayashi, Tomohito, Kuriyama, Shinichi, Matsuda, Shuichi, Tsumaki, Noriyuki, 2015. Generation of Scaffoldless Hyaline Cartilaginous Tissue from Human iPSCs. Stem Cell Rep. 4 (3), 404–418. https://doi.org/10.1016/j.stemcr.2015.01.016.

Yin, Heyong, Wang, Yu, Sun, Zhen, Sun, Xun, Xu, Yichi, Li, Pan, Meng, Haoye, Yu, Xiaoming, Xiao, Bo, Fan, Tian, Wang, Yiguo, Xu, Wenjing, Wang, Aiyuan, Guo, Quanyi, Peng, Jiang, Lu, Shibi, 2016b. Induction of mesenchymal stem cell chondrogenic differentiation and functional cartilage microtissue formation for in vivo cartilage regeneration by cartilage extracellular matrix-derived particles. Acta Biomater. 33, 96–109. https://doi.org/10.1016/j.actbio.2016.01.024.

Yin, Perry T., Han, Edward, Lee, Ki-Bum, 2016a. Engineering Stem Cells for Biomedical Applications. Adv. Healthcare Mater. 5 (1), 10–55. https://doi.org/10.1002/adhm.201400842.

Yurie, H., Ikeguchi, R., Aoyama, T., Kaizawa, Y., Tajino, J., Ito, A., Ohta, S., Oda, H., Takeuchi, H., Akieda, S., Tsuji, M., Nakayama, K., Matsuda, S., 2017. The efficacy of a scaffold-free bio 3D conduit developed from human fibroblasts on peripheral nerve regeneration in a rat sciatic nerve model. PLoS ONE 12. Doi: 10.1371/journal.pone.0171448.

Zhang, Hongji, Voytik-Harbin, Sherry, Brookes, Sarah, Zhang, Lujuan, Wallace, Joseph, Parker, Noah, Halum, Stacey, 2018. Use of autologous adipose-derived mesenchymal stem cells for creation of laryngeal cartilage: ASCs for Creation of Laryngeal Cartilage. Laryngoscope 128 (4), E123–E129. https://doi.org/10.1002/lary.26980.

Zhang, Liangming, Su, Peiqiang, Xu, Caixia, Yang, Junlin, Yu, Weihua, Huang, Dongsheng, 2010. Chondrogenic differentiation of human mesenchymal

stem cells: a comparison between micromass and pellet culture systems. Biotechnol. Lett. 32 (9), 1339–1346. https://doi.org/10.1007/s10529-010-0293-x.
Zhang, Weixiang, Zhu, Yun, Li, Jia, Guo, Quanyi, Peng, Jiang, Liu, Shichen, Yang, Jianhua, Wang, Yu, 2016. Cell-Derived Extracellular Matrix: Basic Characteristics and Current Applications in Orthopedic Tissue Engineering. Tissue Eng. Part B: Rev. 22 (3), 193–207. https://doi.org/10.1089/ten.teb.2015.0290.
Zhao, Chengzhu, Ikeya, Makoto, 2018. Generation and Applications of Induced Pluripotent Stem Cell-Derived Mesenchymal Stem Cells. Stem Cells Int. 2018, 1–8. https://doi.org/10.1155/2018/9601623.
Zhu, Yanxia, Wu, Xiaomin, Liang, Yuhong, Gu, Hongsheng, Song, Kedong, Zou, Xuenong, Zhou, Guangqian, 2016. Repair of cartilage defects in osteoarthritis rats with induced pluripotent stem cell derived chondrocytes. BMC Biotechnol. 16 (1) https://doi.org/10.1186/s12896-016-0306-5.